Published in final edited form as:
Nat Biotechnol. 2008 July ; 26(7): 799–807. doi:10.1038/nbt1415.

An orally delivered small-molecule formulation with antiangiogenic and anticancer activity

Ofra Benny[1], **Ofer Fainaru**[1], **Avner Adini**[1], **Flavia Cassiola**[1], **Lauren Bazinet**[1], **Irit Adini**[1], **Elke Pravda**[1], **Yaakov Nahmias**[2], **Samir Koirala**[3], **Gabriel Corfas**[3], **Robert J D'Amato**[1,4], and **Judah Folkman**[1]

[1] Vascular Biology Program and Department of Surgery, Children's Hospital Boston, Harvard Medical School, 1 Blackfan Circle, St. Karp Research Building, Boston, Massachusetts 02215, USA

[2] Center for Engineering in Medicine, Massachusetts General Hospital, Harvard Medical School, 114 16th Street, Charlestown, Massachusetts 02129, USA

[3] Department of Neurology, F.M. Kirby Neurobiology Center, Children's Hospital, Harvard Medical School, 300 Longwood Avenue, Boston, Massachusetts 02115, USA

[4] Department of Ophthalmology, Harvard Medical School, Children's Hospital Boston, 1 Blackfan Circle, St. Karp Research Building, Boston, Massachusetts 02215, USA

Abstract

Targeting angiogenesis, the formation of blood vessels, is an important modality for cancer therapy. TNP-470, a fumagillin analog, is among the most potent and broad-spectrum angiogenesis inhibitors. However, a major clinical limitation is its poor oral availability and short half-life, necessitating frequent, continuous parenteral administration. We have addressed these issues and report an oral formulation of TNP-470, named Lodamin. TNP-470 was conjugated to monomethoxy-polyethylene glycol–polylactic acid to form nanopolymeric micelles. This conjugate can be absorbed by the intestine and selectively accumulates in tumors. Lodamin significantly inhibits tumor growth, without causing neurological impairment in tumor-bearing mice. Using the oral route of administration, it first reaches the liver, making it especially efficient in preventing the development of liver metastasis in mice. We show that Lodamin is an oral nontoxic antiangiogenic drug that can be chronically administered for cancer therapy or metastasis prevention.

Angiogenesis inhibition has become an important treatment modality for the suppression of tumor growth and metastasis progression[1,2]. TNP-470 is an analog of fumagillin, which was isolated from the fungus *Aspergillus fumigatus fresenius*3 and is among the most potent inhibitors of angiogenesis. In animal models, TNP-470 showed a broad anticancer spectrum

Correspondence should be addressed to O.B. (ofra.bennyratsaby@childrens.harvard.edu).

AUTHOR CONTRIBUTIONS

O.B. designed and developed Lodamin formulation, designed experiments, performed tissue culture, *in vivo* studies and histology, analyzed data and wrote the manuscript; O.F. conducted intrasplenic injections, assisted with editing the manuscript; A.A. and I.A. assisted with cell assays and histology; F.C. conducted TEM imaging and analysis; L.B. assisted with animal studies and conducted corneal assays; E.P. performed confocal microscope imaging; Y.N. performed liver toxicity assays; S.K. and G.C. designed, conducted and analyzed neurotoxicity tests in mice; R.J.D. advised, edited the revisited manuscript and supervised corneal assays. J.F. supervised the entire study, designed experiments, analyzed data and edited the manuscript.

COMPETING INTERESTS STATEMENT

The authors declare competing financial interests: details accompany the full-text HTML version of the paper at http://www.nature.com/naturebiotechnology/.

Published online at http://www.nature.com/naturebiotechnology/
Reprints and permissions information is available online at http://npg.nature.com/reprintsandpermissions/

of activity4. TNP-470 inhibited the growth of primary and metastatic murine tumors and human xenografts such as breast cancer, neuroblastoma, ovarian cancer, prostate cancer, glioblastoma, neurofibrosarcoma and uterine sarcoma and led to a reduction in their vascularization5[−12]. The mechanism of the antiangiogenic activity of TNP-470 is still not completely clear, though proposed molecular mechanisms have suggested targeting methionine aminopeptidase (MetAP-2), affecting cell cycle through p53 activation, induction of p21(CIP/WAF) or preventing Rac1 activation[11,13−15].

TNP-470 was one of the first antiangiogenic drugs to undergo clinical trials[16]. It demonstrated its ability to slow tumor progression or cause durable complete regression17 either given as a single agent, or in combination with other conventional chemotherapeutic drugs such as paclitaxel and carboplatin17−23. The dose-limiting toxicity was neural side-effects such as dizziness, decreased concentration, short-term memory loss, confusion and depression23. Successful elimination of these neurologic symptoms was achieved by the development of Caplostatin (formulated for injection)[24], in which TNP-470 was conjugated to a N-(2-hydroxypropyl)methacrylamide (HPLA) polymer to block penetration of the blood-brain barrier.

Nevertheless, a major clinical limitation of TNP-470 remained unresolved. The poor oral availability of TNP-470 coupled with its extremely short plasma half-life imposes a strict regime of prolonged parenteral administration23,[25]. TNP-470 needs to be administered frequently as continuous intravenous infusions (usually over 1 h, multiple times a week) in the clinic. Therefore, developing an oral formulation may considerably improve patient compliance and provide means for a long-term antiangiogenic therapy for cancer and other angiogenesis-dependent diseases.

In this work we report an oral antiangiogenic polymeric drug with potent antitumor and antimetastatic efficacy named Lodamin. We characterize the physicochemical properties and show that this formulation of TNP-470 overcomes the drug's limitations while retaining its antiangiogenic activity. Lodamin is produced by conjugation of TNP-470 to a di-block copolymer, monomethoxy-polyethyleneglycol–polylactic acid (mPEG-PLA). The amphiphilic nature of this polymeric drug enables self-assembly of micelles in an aqueous medium[26]. In this structure, the TNP-470 is located in the core, where it is protected from the acidic environment of the stomach, thus enabling oral availability. Furthermore, we take advantage of using biocompatible, commonly used and well-characterized polymers27,28.

Our results indicate that Lodamin, administered orally, is effectively absorbed in the intestine and accumulates in tumor tissue. The drug significantly inhibits angiogenesis, as demonstrated by inhibition of human umbilical vein endothelial cell (HUVEC) proliferation, by the corneal micropocket assay and in mouse tumor models. Lodamin significantly inhibited primary tumor growth as demonstrated in models of melanoma and lung cancer. Notably, oral Lodamin successfully prevented liver metastasis of melanoma tumor cells without causing liver toxicity or other side effects and prolonged mouse survival.

Unlike free TNP-470, Lodamin does not penetrate the blood-brain barrier and accordingly did not cause neurotoxicity in mice. These results suggest that Lodamin may be a good candidate for a safe maintenance drug with effective antitumor and antimetastatic properties.

RESULTS

Chemical and physical characterization of Lodamin

To predict the oral availability of TNP-470, we measured its hydrophobicity using the log-D parameter. The measured log-D values were 2.39 at pH = 2 and 2.57 at pH = 7.4. The high log-

D values (>2) indicate very low solubility in water. This property led us to design a formulation with improved solubility and oral availability.

We characterized the chemical and physical properties of Lodamin. We confirmed the binding of TNP-470 to mPEG-PLA by ^{3}H NMR (data not shown) and mass spectrometry showing an average *m*/*z* of 3,687 for mPEG-PLA-TNP-470. Figure 1a illustrates the preparation of Lodamin. Using an amine detection reagent, we determined the incorporation efficiency of ethylenediamine to mPEG-PLA as 65%, and in the second step TNP-470 was shown to be bound with an efficiency of >90%. Lodamin contained 0.8–1% (wt/wt) free TNP-470 as determined by high-performance liquid chromatography (HPLC). We determined the average size and size distribution of Lodamin by dynamic light scattering (DLS) spectroscopy (Fig. 1b) on the day of preparation and after 10 d of incubation in aqueous medium, to evaluate Lodamin stability ($n = 4$). The majority of micelles (90%) on the day of preparation were 7.8–8 nm in diameter, with a small population of larger particles (200–400 nm). The size remained almost unchanged after 10 d.

We characterized the morphology of Lodamin by transmission electron microscopy (TEM) (Fig. 1c). The images showed that the polymeric micelles had acquired a uniform spherical structure, which remained stable after 2 weeks of incubation in water at 37 °C. Because the drug is located in the PLA core of the micelle structure and PLA is spontaneously hydrolyzed in an aqueous environment, we studied the release kinetics of TNP-470 from Lodamin. A slow-release kinetic of TNP-470 was obtained after incubation in PBS (pH = 7.4) or in gastric liquid (pH = 1.2). The TNP-470 was released over a period of 28 d with an early peak burst of ~30% after the first day of incubation (Fig. 1d).

Endothelial cells take up Lodamin by endocytosis

We evaluated the uptake of polymeric micelles by HUVECs and the kinetics of their uptake. HUVECs were incubated with 6-coumarin labeled mPEG-PLA micelles for 20 min, 2, 4 and 7 h and were imaged by confocal microscopy (Fig. 2a). In as little as 20 min after incubation, micelles were taken up by the cells and located in their cytoplasm. After 2 h the uptake was maximal and after 4–7 h micelles were detected as defined aggregates inside the cytoplasm. Fluorescence-activated cell sorting (FACS) of HUVECs incubated with rhodamine-labeled polymeric micelles for the same incubation times confirmed a maximal uptake after 2 h (Fig. 2b), whereas no difference was observed between 2 and 24 h of incubation. In live-cell analysis, co-localization of Lyso-tracker staining with the micelles suggests endocytosis as the mechanism of uptake. Incubation of the micelles with HUVECs in cold conditions reduced micelle uptake by up to 55%, confirming that endocytosis is the most likely mechanism of uptake (data not shown).

Lodamin inhibits proliferation of endothelial cells

Next, we evaluated the effect of Lodamin on the proliferation of endothelial cells. After 48 h, Lodamin (62.5 nM–1,000 nM TNP-470 equivalent) inhibited HUVEC proliferation by 88–95% respectively (Fig. 2c). The growth of HUVECs treated with Lodamin (60 nM TNP-470 equivalent) was completely inhibited compared to untreated cells or cells treated by vehicle only. We observed no substantial cytotoxic effect (Fig. 2c).

Lodamin inhibits bFGF and VEGF-induced angiogenesis *in vivo*

The antiangiogenic properties of Lodamin were evaluated *in vivo* by the corneal micropocket angiogenesis assay[29]. Mice were treated with daily oral Lodamin (15 mg/kg per day) or vehicle for 6 d. Figure 2d shows the inhibition of basic fibroblast growth factor (bFGF)-induced angiogenesis in representative eyes of treated or untreated mice. Quantification of the angiogenesis area (Fig. 2d, lower panel) showed 31% inhibition of angiogenesis, compared to

vehicle ($P = 0.00016$, $n = 10$). Similar results were obtained with 160 ng vascular endothelial growth factor $(VEGF)_{165}$-induced angiogenesis in the cornea (data not shown); in this case Lodamin treatment resulted in 40% inhibition of vessel area.

Polymeric micelles: absorption by the intestine

To study the intestinal absorption of the polymeric-micelles, we orally administered mPEG-PLA-rhodamine micelles to mice. After 2 h mice were euthanized and isolated segments of the small intestine were fixed and imaged using confocal microscopy. The polymeric micelles (detected in the red channel) were intensively taken up by columnar epithelium lining the luminal side of the small intestine (Fig. 3a). In a high magnification of small intestine villi, micelles are clearly detected in the lamina propria and in the vicinity of blood vessels, indicating transepithelial absorption. In high-resolution TEM images of single gut-epithelial cells, endosomes loaded with drug were readily detected (Fig. 3a, arrows). These endosomes differed in contrast and number when compared to those in the intestine of an untreated mouse. These data indicate that Lodamin is most likely taken up by intestinal villi through endocytosis.

Biodistribution, tumor accumulation and toxicity studies

The biodistribution and tissue uptake of orally administered labeled Lodamin was studied by treating mice with fluorescently labeled mPEG-PLA micelles for 3 d. After harvesting tissue, we quantified tissue drug concentration by dye extraction or by FACS. The results of the fluorescent dye extraction method (Fig. 3b) showed that a high concentration of fluorescent signal was present in the stomach and the small intestine, and the highest levels were present in the liver. Notably, the brain lacked fluorescent signal. In the serum, labeled micelles were already detected 1 h after oral administration, peaking after 2 h and were still detected at 72 h. In tumor-bearing mice, FACS analysis of enzymatically digested tissues (Fig. 3c,d) demonstrated a large uptake of labeled micelles by the liver, and no uptake by the brain. Notably, the highest uptake of micelles was detected in tumor cells (Fig. 3c). Taken together, these results indicate that the drug was concentrated mostly in the tumor and to a lesser extent in the gastrointestinal organs, and absent in the brain.

No tissue abnormalities were detected by histological analyses (H&E) of liver, intestine, lung and kidney in Lodamin-treated mice (15 mg/kg TNP-470 equivalent per day, for 20 d) compared to untreated mice (data not shown). In addition, no substantial differences were found between the mouse serum liver-enzyme profiles of Lodamin-treated and untreated mice. In the Lodamin-treated group the aspartate aminotransferase (AST) and alanine aminotransferase (ALT) concentrations were 41 ± 9 u/l and 120 ± 39 u/l, respectively, whereas in the untreated group they reached 37.5 ± 4 u/l and 152 ± 131 u/l, respectively.

Lodamin inhibits primary tumor growth

We evaluated the biological efficacy of Lodamin as an antiangiogenic anticancer agent in tumor-bearing mice. When mice received an oral dose of free TNP-470 (30 mg/kg every other day), we did not observe tumor growth inhibition in subcutaneous Lewis lung carcinomas (LLC) (Fig. 4a). The equivalent dose of Lodamin, however, resulted in substantial tumor growth inhibition (Fig. 4a). This inhibition was observed after 12 d of Lodamin treatment, and at day 18 tumor growth was inhibited by 83%. Different dosing regimens of Lodamin, 15 mg/kg every day, 30 mg/kg every other day and 15 mg/kg every other day, resulted in 87%, 77% and 74% inhibition of tumor volume, respectively (Fig. 4b). The vehicle (mPEG-PLA) showed no effect on tumor growth and was similar to untreated control mice (Fig. 4c).

In another tumor model, murine melanoma (B16/F10) subcutaneous tumor growth was also inhibited by oral Lodamin (15 mg/kg per day). This treatment was effective after 4 d of treatment, and after 13 d, 77% volume inhibition was obtained (Fig. 4d). No apparent side

effects, including weight loss, were detected in either tumor model. Higher doses of Lodamin —30 mg/kg per day and 60 mg/kg every other day—showed substantial tumor inhibition; however, these higher doses were accompanied by weight loss (data not shown). Figure 4e shows representative tumors of treated or untreated LLC or B16/F10 tumors.

Lodamin does not cause neurotoxicity in mice

Because our biodistribution study indicated that Lodamin does not cross the blood-brain barrier, we tested whether the possible leaching of free drug into the brain might result in neurotoxicity and cerebellar dysfunction. We subjected mice to a sensitive test of motor coordination—crossing a narrow (4 mm) balance beam[30]. The performance of Lodamin-treated mice (30 mg/kg TNP-470 equivalent every other day for 14 d) was similar to that of control (water-treated) mice, whereas mice injected with the same dose of free TNP-470 committed over twice as many errors ($P < 0.0001$) (Fig. 4f). These results indicate that Lodamin treatment avoids the cerebellar neurotoxicity observed with unconjugated TNP-470 treatment.

Lodamin inhibits tumor angiogenesis and proliferation

We tested the effect of Lodamin on the histological structure of LLC tumors. Both treated and untreated tumors showed a dense cellular structure (Fig. 5). The tumors of untreated mice had a net organization of small and large vessels with an apparent lumen structure as demonstrated by CD-31 immunostaining. In contrast, Lodamin-treated tumors formed very small undeveloped vessels (Fig. 5). Lodamin-treated tumors showed less cellular proliferation than untreated tumors, as detected by the nuclear marker Ki-67. TdT-mediated dUTP nick end labelling (TUNEL) staining for the detection of apoptosis suggested enhanced apoptosis in Lodamin-treated tumors. Lodamin-treated tumors had fewer vessels (green) but high levels of apoptosis, predominantly in tumor cells (red). In the control tumor tissue, apoptotic cells were mostly found in the capsule and less in the center.

Lodamin prevents development of liver metastasis

The effect of oral Lodamin administration on liver metastases was tested after injecting B16/F10 tumor cells into the spleen. Oral Lodamin treatment dramatically affected development of B16/F10 liver metastasis. After 18 d of treatment mice were autopsied. All untreated mice had ascites and their enlarged livers had macroscopic malignant nodules and extensive cirrhosis (Fig. 6a,b). In contrast, Lodamin-treated mice had no macroscopic metastases in the abdomen or in the liver (Fig. 6a,b). Their organs had a normal morphology and no weight loss or other apparent side effects were found. Immunohistology showed only a few sporadic B16/F10 cells in the liver that had not developed into lesions (Fig. 6b). Only one treated mouse out of seven had malignant nodules in its liver, but the liver was smaller than in the untreated control and had less cirrhosis. The spleens of all Lodamin-treated mice had a normal morphology compared to the congestion found in the enlarged spleens of control mice (Fig. 6c). Twenty days after B16/F10 cell injection into the spleen, four out of seven control mice had died whereas all treated mice survived (Fig. 6d).

DISCUSSION

In cancer patients, tumor- and micrometastasis can remain for prolonged periods of time in a dormant asymptotic state before diagnosis and development of disease[1,31]. Recent advances in identifying biomarkers of the "angiogenic switch"[2,32–34] may open new possibilities for early detection of dormant tumors. Dormancy highlights the need for chronic long-term therapy with nontoxic anticancer drugs preferentially administered orally.

In this study, we describe the development of a nontoxic oral formulation of TNP-470, named Lodamin, as an antitumor and antimetastatic drug. We chose this drug because TNP-470, a

highly potent angiogenesis inhibitor, is a reasonable candidate for cancer maintenance therapy and metastasis prevention.

In the current study we devised a soluble formulation for TNP-470, a molecule with very poor oral availability as illustrated by its high log-D values, indicating low water solubility[35]. We made an oral formulation by conjugating TNP-470 with mPEG-PLA to form mPEG-PLA-TNP-470 polymeric micelles. Unlike TNP-470, which is only dissolvable in organic solvents, Lodamin can be suspended in water to form polymeric micelles thanks to the amphiphilic nature of PEG-PLA[26]. In this structure the drug is located in the core of the micelle, protecting it from the harsh gastrointestinal environment[36]. Polymer micelles have previously been used for the delivery of hydrophobic drugs[37,38] and gene delivery[39].

TEM indicated that Lodamin acquired a stable spherical morphology of nanomicelles. In addition, PLA, a biodegradable and biocompatible polymer, hydrolyzes in an aqueous environment and allows slow release of TNP-470. *In vitro* studies showed a continuous release of TNP-470 from Lodamin over almost a period of 1 month, with the majority of the drug releasing within the first 4 d (in both gastric and plasma pH conditions). Although an acidic environment is known to accelerate degradation of PLA, we observed only a minor effect on day 15. One possible explanation may be the masking effect of the PEG shell, which delays water penetration to the PLA core and slows diffusion-mediated release of the drug through this layer. In culture, Lodamin was rapidly taken up by endothelial cells via endocytosis and retained the original antiangiogenic activity of the free TNP-470 as demonstrated by the inhibition of HUVEC proliferation.

mPEG-PLA micelles penetrated the gut epithelial layer into the submucosa as shown by using fluorescent markers. The mechanism of Lodamin penetration to gut epithelial cells seems to be by endocytosis, as detected by high-resolution TEM. In serum, labeled micelles had a long blood circulation time of at least 72 h after administration, a significant increase compared to free drug, which was detected in mice sera up to 2 h after treatment[24]. Biodistribution showed relatively high concentrations in the liver, as oral administration directly delivers the drug from the intestine to the liver. However, no liver toxicity was observed by histology and by liver enzyme profiling after 20 d of daily Lodamin treatment.

Orally delivered Lodamin showed substantial antitumor effects (83% reduction), whereas orally administered free TNP-470 had no effect. The effect on LLC growth was dose dependent, as 30 mg/kg every other day was more effective than 15 mg/kg every other day, and a dose of 15 mg/kg daily was more effective than 30 mg/kg every other day (a double dose given every 2 d). A similar antitumor effect of Lodamin was observed with melanoma B16/F10 tumors, confirming the broad biological effect of Lodamin, very much like the original free TNP-470. Immunohistochemical studies carried out on LLC tumor tissues showed Lodamin-induced reduction of proliferation and angiogenesis. TUNEL staining indicated a high level of tumor cell apoptosis after treatment. These results suggest that the prevention of angiogenesis by Lodamin leads to tumor cell apoptosis.

One of the most important effects of oral Lodamin is the prevention of liver metastasis in mice. Liver metastasis is very common in many tumor types and is often associated with a poor prognosis and survival rate. We chose the intrasplenic model for induction of liver metastasis, in which the transition time of B16/F10 cells from the spleen to the liver microvasculature was found to be very fast (20% of the injected cells are located in the liver after 15 min)[40]. Mice injected in the spleen with B16/F10 cells had a low survival rate. They developed ascites, macroscopic malignant nodules and extensive cirrhosis in their livers 20 d after injection. However, all oral Lodamin–treated mice survived up to this point and had a normal liver and spleen morphology without any apparent side effects. This dramatic antitumor effect in the

liver may be due to the oral route of administration in which Lodamin is absorbed in the gastrointestinal tract and concentrated in large quantities in the liver via the portal vein. These results suggest that Lodamin can prevent the development of metastasis in the liver. Importantly, this property of the polymeric micelles might be used for the development of other antiangiogenic or anticancer drugs that target liver metastasis.

In tumor-bearing mice, Lodamin showed preferential accumulation in the tumor rather than in other tissues. This accumulation may be due to the enhanced permeability and retention effect (EPR) caused by the 'leaky' discontinuous endothelium of the tumor vasculature[41]. The EPR effect plays a central role in nanoparticle targeting to tumor beds, as in the case of Caplostatin24 and other conjugated drugs42. Furthermore, biodistribution studies showed that polymeric micelles do not penetrate the brain through the blood-brain barrier. Because TNP-470 was shown to cause neurotoxic side-effects in humans in clinical trials23, we examined whether Lodamin treatment caused neurotoxicity and cerebellar dysfunction in treated mice. In the narrow beam test, mice injected with free TNP-470 showed a substantial increase in foot-slip errors, whereas Lodamin-treated mice performed like untreated control mice.

In summary, oral Lodamin shows promising therapeutic properties in the treatment of solid tumors and metastasis in mice. It retains the antiangiogenic properties of free TNP-470 while adding important advantages: oral availability, tumor accumulation, continued slow release and fewer side effects. It may be useful for cancer patients as a long-term maintenance drug to prevent tumor recurrence. Furthermore, it may be used as a maintenance therapy for chronic angiogenic diseases such as age-related macular degeneration, endometriosis and rheumatoid arthritis.

METHODS

All animal procedures were performed in compliance with Boston Children's Hospital guidelines, and protocols were approved by the Institutional Animal Care and Use committee.

Log-D measurement for TNP-470

Aqueous solubility is one of the important chemical properties affecting oral absorption of a drug. In order to predict the intestinal absorption of TNP-470, we measured its log-D value which is a parameter of hydrophobicity determined by the ratio of drug concentration in octanol to that in water at 25 °C (Analiza). High log-D values (>2) indicate low water solubility and hence a poor oral availability of a drug. For this study log-D values of TNP-470 (30 mM) were measured at plasma and stomach pHs: pH = 7.4 and pH = 2, respectively.

Preparation of Lodamin: mPEG-PLA-TNP-470 polymeric micelles

TNP-470 (D. Figg) was conjugated to a diblock co-polymer using a two-step reaction (Fig. 1). In the first step succinated $mPEG_{2000}$-PLA_{1000} with free carboxic acid end-groups (Advanced Polymers Materials) was reacted with ethylenediamine (Sigma-Aldrich). Succinated mPEG-b-PLA-$OOCCH_2CH_2COOH$ (500 mg) was dissolved in DMSO and reacted with ethyl (diethylaminopropyl) carbodiimide (EDC) and a catalyst *N*-hydroxysuccinimide (NHS) in a molar ratio of 1:10:20 (Polymer:EDC:NHS, respectively). A fivefold molar excess of ethylendiamine was added and reacted for 4 h at 25 °C. The polymer solution was then dialyzed (MWCO 1000, Spectra/Por Biotech Regenerated Cellulose, VWR) against DMSO leading to a 65% reaction efficiency. In the second step, the amine-containing polymer was mixed with TNP-470 (350 g), dissolved in DMSO and the solution was stirred for 4 h at 25 °C. The polymeric micelles were formed by dialyzing the DMSO solution of the conjugate against double distilled water (d.d.w.) using a regenerated cellulose dialysis bag (MWCO 1000,

Spectra/Por Biotech Regenerated Cellulose, VWR) to obtain micelles with high incorporation efficiency (>90%) and 0.8–1% free drug (wt/wt). The micelles were then lyophilized and stored at −20 °C in a dry environment until use.

Prepartion of fluorescently labeled mPEG-PLA micelle

Rhodamine-labeled polymeric-micelles were formed using a similar protocol. The mPEG-PLA was conjugated via the N-terminal amine group with lissamine rhodamine B sulfonyl chloride (Molecular Probes) in DMSO. For green fluorescent polymer micelles, a commonly used hydrophobic marker 6-coumarin (Sigma-Aldrich) at 0.1% wt/wt was added to the polymeric solution before the final dialysis step.

Characterization of conjugation

NMR spectrometer analysis (NERCE/BEID, Harvard Medical School) was conducted for each reaction step and mass spectrometry (Proteomic core, Harvard Medical School) was performed on the conjugate. To evaluate the efficiency of ethylendiamine binding to mPEG-PLA (first reaction step, Fig. 1a) and TNP-470 binding to the polymer by the amine (second step, Fig. 1a), we used the colorimetric amine detection reagent: 2,4, 6-trinitrobenozene sulfonic acid (TNBSA) (Pierce). TNBSA reacts with primary amines to produce a yellow product whose intensity was measured at 450 nm. To calculate amine concentration in the polymer a linear calibration curve of amino acid was used. To measure TNP-470 loading into polymeric micelles, we incubated 10 mg/ml Lodamin in 500 μl NaOH (0.1 N) to accelerate PLA degradation. After an overnight incubation with shaking (100 r.p.m) at 37 °C, we added acetonitrile to the samples (1:1 NaOH:acetonitrile) and analyzed for TNP-470 concentration. TNP-470 concentration was measured using HPLC (System Gold Microbore, Beckman Coulter). A 20-μl portion of each sample was injected into a Nova-pak C_{18} column (3.9 mm × 150 mm i.d.; Waters) and analyzed using a calibration curve of TNP-470. TNP-470 binding to amine was also measured using TNBSA reagent and was confirmed by subtracting the nonbound drug from the total drug added to the reaction.

Lodamin size, morphology and *in vitro* TNP-470 release

The particle size distribution of Lodamin was measured by Dynamic Light Scattering (DLS, DynaPro, Wyatt Technology). The measurements were done at 25 °C using Dynamic V6 software. Lodamin (1.5 mg/ml) dispersed in d.d.w. was measured in 20 successive readings of the DLS.

To study the morphology of Lodamin, TEM images were taken on the day of preparation and 1 week after preparation. Polymer micelles dispersed in d.d.w. were imaged with cryo-TEM (JEOL 2100 TEM, Harvard University—CNS). To study the kinetic release of TNP-470 (without its chlorine), Lodamin (20 mg) was incubated with either 1 ml PBS pH = 7.4 or simulated gastric fluid (HCL:d.d.w. pH = 1.2). Every few days, supernatant was taken and analyzed for TNP-470 concentration and a cumulative release graph of TNP-470 was determined. TNP-470 concentration was measured using HPLC. TNP-470 was detected as a peak at 6 min with 50% acetonitrile in water at the mobile phase. The flow rate was 1 ml/min, and the detection was monitored at 210-nm wavelength.

Cell culture

Murine LLC and B16/F10 melanoma cells were obtained from American Type Culture Collection. HUVECs were purchased from Cambrex. The cells were grown and maintained in medium as recommended by the manufacturers. Dulbecco's Modified Eagle's Medium with 10% FBS was used for tumor cells and EMB-2 (Cambrex Bio Science) containing 2% FBS and EGM-2 supplements was used for HUVECs.

Uptake of polymeric micelles by HUVECs and their localization in cells

To evaluate the uptake of polymeric micelles by HUVEC, we used 6-coumarin-labeled mPEG-PLA micelles or rhodamine conjugated to mPEG-PLA. HUVECs were seeded in a 24-well plate (2×10^4 per well) in EGM-2 medium (Cambrex) and were allowed to attach overnight. Fluorescent-labeled micelles (10 mg/ml) were suspended over a bath sonicator for 5 min, and 20 μl of the suspension was added to the cultured cells. After the designated time points (20 min, 2, 4, 7 and 24 h), the cells were washed three times with PBS and analyzed by FACS or alternatively fixed with 4% parformaldehyde. For confocal microscopy, cells were mounted using DAPI containing Vectashild (Vector Laboratories). Optical sections were scanned using Leica TCS SP2 AOBS, a ×40 objective equipped with 488-nm argon, 543-nm HeNe and 405-nm diode lasers. To study Lodamin internalization into endothelial cells, we used confocal microscopy to co-localize 6-coumarin–labeled polymeric micelles with endolysozome. Live HUVECs were imaged in different time points after addition of labeled micelles to cell medium (15 μg/ml) up to 1 h. At this point, LysoTracker Red (Molecular Probes) was added to the medium for the detection of acidic intracellular vesicles: endosomes and lysosomes. After 20 min of incubation, cells were imaged by confocal microscopy using optical sections with 488-nm argon, 543-nm HeNe and 405-nm diode lasers.

To further verify that Lodamin internalization occurs through endocytosis, we measured cell uptake in cold conditions (4 °C) in comparison to cell uptake at 37 °C. HUVECs were plated in a concentration of 15,000 cells/ml in two 24-well plates for 24 h. Fluorescence-labeled polymeric micelles (15 μg/ml) were added and incubated at different time points: 20, 30, 40 and 60 min ($n = 3$) in 4 °C and in 37 °C. After the designated time points, the cells were washed three times with PBS and lysed with 100 μl lysis buffer (BD Biosciences). Cell extracts were measured for fluorescent signal in a Wallac 1420 VICTOR plate-reader (Perkin-Elmer Life Sciences) with excitation/emission at 488 nm/530 nm.

HUVEC growth and proliferation

HUVECs were exposed to different concentrations of Lodamin equivalent to 50–1,000 nM free TNP-470 (0.12–2.4 mg/ml micelles) and incubated in a low serum medium for 48 h at 37 °C. To rule out a possible cytotoxic effect of the carrier, empty micelles were added to HUVECs at the same concentration as the control (4.8 mg/ml). A WST-1 proliferation assay (Roche Diagnostics) was used. Cell viability was calculated as the percentage of formazan absorbance at 450 nm of treated versus untreated cells. Data were derived from quadruplicate samples in two separate experiments. The effect of Lodamin (60 nM TNP-470 equivalent every other day) on HUVEC growth rate was evaluated by daily counting of HUVECs up to 5 d and comparing this to the number of untreated cells or cells treated with vehicle (same concentration as Lodamin).

Corneal micropocket assay

To evaluate the antiangiogenic properties of Lodamin, the corneal micropocket angiogenesis assay was performed as previously detailed[29]. Pellets containing 80 ng carrier-free recombinant human bFGF or 160 ng VEGF (R&D Systems) were implanted into micropockets created in the cornea of anesthetized mice. Mice were treated daily with 15 mg/kg TNP-470 equivalent of Lodamin for 6 d, and then the vascular growth area was measured using a slit lamp. The area of neovascularization was calculated as vessel area by the product of vessel length measured from the limbus and clock hours around the cornea, using the following equation: vessel area (mm^2) = ($\pi \times$ clock hours $\times$ vessel length (mm) $\times$ 0.2 mm).

Body distribution, intestinal absorption and toxicity of Lodamin

For all biodistribution studies we used a fluorescent marker for tracking Lodamin. Mice were administered 6-coumarin–labeled mPEG-PLA by oral gavage for 3 d (100 μl of 1.5 mg/ml). On the third day of treatment, after 8 h of fasting, animals were killed and spleen, kidney, brain, lungs, liver, intestine, stomach and bladder were collected. The fluorescent 6-coumarin was extracted from the tissues by incubation with formamide for 48 h at 25 °C. Samples were centrifuged and signal intensity of fluorescence of supernatants was detected with a Wallac 1420 VICTOR plate-reader (Perkin-Elmer Life Sciences) with excitation/emission at 488 nm/530 nm. The results were normalized to protein levels in the corresponding tissues. Tissue autofluoresence was corrected by subtracting the fluorescent signal of nontreated mouse organs from the respective readings in treated mice. Similarly, levels of fluorescent signal in mouse sera were measured at different time points (1, 2, 4, 8, 24, 48 and 72 h) using excitation/emission readings at 488 nm/530 nm.

To analyze cell uptake in the different tissues in tumor-bearing mice, we administered orally mPEG-PLA-rhodamine micelles (100 μl of 1.5 mg/ml) or water to C57Bl/6J mice bearing LLC tumors (200 mm^3) for 3 d. Organs were removed, incubated for 50 min in collagenase (Liberase Blendzyme 3; Roche Diagnostics) in 37 °C to obtain a single-cell suspension. These suspensions were analyzed by FACS to quantify the uptake of micelles into different tissue cells when compared to those in the untreated mouse.

To evaluate intestinal absorption, mPEG-PLA-rhodamine micelles were orally administered to C57Bl/6J mice after 8 h of fasting. After 2 h mice were killed and 2.5-cm segments of the small intestine were removed, washed and analyzed by histology and confocal microscopy. The rhodamine-labeled polymeric micelles were detected by confocal microscopy (Leica TCS SP2 AOBS) with a 488-nm argon laser line. Actin filaments were stained with phalloidin-FITC (Sigma) and nuclei were stained by DAPI (Sigma). To further study the uptake of Lodamin in the intestine, high-resolution images were made with cryo-TEM. Intestines from treated (as above) and untreated mice were excised and immersed immediately in a freshly prepared 4% paraformaldehyde in PBS pH 7.4 for 2 h at 25 °C. The samples were washed in PBS, transferred to a 30% sucrose solution overnight at 4 °C and embedded in OCT and kept at −80 °C until processing. Fifteen sections, each 10 μm thick, were prepared and processed for confocal microscopy or TEM. Four TEM samples were fixed for 30 min in freshly prepared 2% paraformaldehyde, 2.5% glutaraldehyde, 0.025% CaCl2 in 0.1 M sodium cacodylate buffer, pH 7.4 and subsequently postfixed for 30 min in 1% osmium tetroxide in 0.1 M sym collidine buffer, pH 7.4 at 25 °C, stained *en bloc* in 2% uranyl acetate, dehydrated and embedded under inverted plastic capsules. Samples were snapped free of the glass cover-slips by a cycle of rapid freezing and thawing. Thin sections were cut *en face* with diamond knives using a LEICA UCT Ultramicrotome. Specimens were examined using a JEOL 2100 TEM.

To exclude tissue toxicity, histological analysis (H&E) of liver, intestine, lung and kidneys was conducted (Beth-Israel pathology department). To further exclude liver toxicity, we analyzed serum levels of the liver enzymes AST and ALT (done at Shriners Burns Hospital). These studies were performed on mice treated with Lodamin for 20 d (15 mg/kg TNP-470 equivalent per day) and compared to untreated mice (n = 3–4).

Oral administration of Lodamin *in vivo* and primary tumor experiments

Animal procedures were performed in the animal facility at Children's Hospital Boston using 8-week-old C57Bl/6J male mice (Jackson Laboratories).

For tumor experiments: LLC cells (1×10^6) or B16/F10 melanoma cells (1×10^6) were implanted subcutaneously in 8-week-old C57Bl/6J male mice. Oral availability of free

TNP-470 was compared to that of Lodamin. A dose of 30 mg/kg every other day of free TNP-470 and an equivalent dose of Lodamin (Lodamin, 6 mg in 100 μl/d per mouse) were administered to LLC tumor-bearing mice (~100 mm^3) and tumor growth was followed for 18 d. Free drug was given as a suspension in d.d.w. and freshly prepared before each dose. Additionally, we compared different doses and frequencies of Lodamin treatment: 15 mg/kg every day, 15 mg/kg every other day and 30 mg/kg every other day. To eliminate any possible effect of the vehicle (polymer without drug), we gave one group of mice micelles without drug and tumor progression was compared to water-treated mice.

For the melanoma tumor experiment, a daily dose of 15 mg/kg Lodamin was administered to B16/F10 melanoma-bearing mice. In all experiments, tumor size and animal weight were monitored every 2 d. Tumor volume was measured with calipers in two diameters as follows: $(\text{width})^2 \times (\text{length}) \times 0.52$. Note that all the above Lodamin doses are presented as TNP-470 equivalent.

Oral administration of Lodamin and liver metastasis experiments

To examine the effect of oral Lodamin treatment on metastasis development and prevention, liver metastases were generated by spleen injection. C57Bl/6J mice ($n = 14$) were anaesthetized with isoflurane and prepared for surgery. A small abdominal incision was made in the left flank and the spleen was isolated. B16/F10 tumor cells in suspension (50 μl, 5×10^5 in DMEM medium without serum) were injected into the spleen with a 30-gauge needle, and the spleen was returned to the abdominal cavity. The wound was closed with stitches and metal clips. After 2 d mice were divided into two groups: one was treated daily with oral Lodamin (15 mg/kg) using gavage and the second group was administered water by gavage. After 20 d, we terminated the experiment. Mice were killed and autopsied, livers and spleens were removed by surgical dissection, imaged and histology was carried out. Liver and spleen tissues were stained with H&E to evaluate tissue morphology and detect metastasis. Immunohistochemistry was carried out to specifically detect B16/F10 cells in the liver using anti-mouse melanoma antibody (HMB45, abCAM) and using DAB staining.

Evaluation of neurotoxicity with balance beam motor coordination test

A slightly modified balance beam motor coordination test[30] was performed on three groups of mice: oral Lodamin–treated mice (30 mg/kg eq. every other day), free TNP-470 (30 mg/kg every other day) subcutaneously injected mice and water-treated mice (administered by gavage). The mice were pretreated for 14 d ($n = 4$–5 per group) and then the mice were allowed to acclimate to the procedure room for 1 h, after which they were trained in three trials to cross a wide (20 mm width × 1 m length) balance beam. All the mice crossed the wide beam without making foot-slip errors. The mice were then trained on a narrow (4 mm width × 1 m length) beam for three trials. At the end of the training trials, no freezing behavior was observed, and the mice would start to walk within 4 s of being placed on the beam. The mice were then videotaped as they performed in three test trials of three beam crossings each—a total of nine crossings per mouse. The three trials were separated by at least 1 h to avoid fatigue of the mice. Videotaped crossings were scored for number of foot-slip errors and time to cross. All experiments and scoring of the different groups were performed by a blinded investigator.

Lodamin effect on angiogenesis, proliferation and apoptosis in tumor tissues

Histologic evaluation of tissue was performed on 8-μm thick frozen sections of LLC tumors that were removed from two random Lodamin-treated or untreated mice 14 d after treatment (15 mg/kg every day. TNP-470 equivalent). Tumors were sectioned and analyzed for cell markers, 20 microscope fields (×400) were imaged.

Tissues were stained with H&E to detect tissue morphology. Immunohistochemistry was carried out using Vectastain Elite ABC kit (Vector Laboratories). Primary antibodies included CD31 (BD Biosciences) for microvessel staining and anti-Ki-67 (DAKO) for proliferating cell. Detection was carried out using a 3,3′-diaminobenzidine chromogen, which results in a positive brown staining. Apoptotic cells were detected by reacting the tissues with TUNEL using a kit (Roche) following the company's protocol. Vessels were detected in the same tissues by anti-CD31 and secondary FITC anti-mouse antibody (Jackson ImmunoResearch) conjugated antibody (green) and nuclei were detected by DAPI (blue).

Statistics

In-vitro data are presented as mean ± s.d., whereas *in vivo* data are presented as mean ± s.e.m. Differences between groups were assessed using unpaired two-tailed Student's *t*-test, and $P < 0.05$ was considered statistically significant.

Acknowledgments

We thank Donald Ingber for his support and encouragement of this work, Daniela Prox and Jenny Mu for their assistance with animal studies and chemical analysis, Kristin Johnson for the graphic work, Chun Wang (University of Minnesota) for fruitful discussions. We thank D. Figg, National Cancer Institute, for TNP-470. This work is supported in part by a Department of Defense Congressional Award W81XWH-05-1-0115 (to J.F.). The submission of this paper was completed before Folkman passed away in January and is dedicated to him for his support and mentorship.

References

1. Holmgren L, O'Reilly M, Folkman J. Dormancy of micrometastases: balanced proliferation and apoptosis in the presence of angiogenesis suppression. Nat Med 1995;1:149–153. [PubMed: 7585012]
2. Naumov, G.; Folkman, J. Strategies to prolong the nonangiogenic dormant state of human cancer. In: Darren, W.; Herbst, RS.; Abbruzzese, JL., editors. Antiangiogenic cancer therapy. Vol. 1. CRS Press; Boca Raton, FL, Taylor and Francis: 2007. p. 3-23.
3. Ingber D, et al. Synthetic analogue of fumagillin that inhibit angiogenesis and suppress tumour growth. Nature 1990;348:555–557. [PubMed: 1701033]
4. Folkman, J.; Kalluri, R. Tumor angiogenesis. In: Kufe, D., et al., editors. Cancer Medicine. Vol. 1. B.C. Decker Inc; Hamilton, Ontario: 2003. p. 161-194.
5. Yamaoka M, Yamamoto T, Ikeyama S, Sudo K, Fujita T. Angiogenesis inhibitor TNP-470 (AGM-1470) potently inhibits the tumor growth of hormone-independent human breast and prostate carcinoma cell lines. Cancer Res 1993;53:5233–5236. [PubMed: 7693335]
6. Shusterman S, et al. The angiogenesis inhibitor tnp-470 effectively inhibits human neuroblastoma xenograft growth, especially in the setting of subclinical disease. Clin Cancer Res 2001;7:977–984. [PubMed: 11309349]
7. Yanase T, Tamura M, Fujita K, Kodama S, Tanaka K. Inhibitory effect of angiogenesis inhibitor TNP-470 on tumor growth and metastasis of human cell lines in vitro and in vivo. Cancer Res 1993;53:2566–2570. [PubMed: 7684319]
8. Takamiya Y, Brem H, Ojeifo J, Mineta T, Martuza R. AGM-1470 inhibits the growth of human glioblastoma cells in vitro and in vivo. Neurosurgery 1994;34:869–875. [PubMed: 8052385]
9. Takamiya Y, Friedlander RM, Brem H, Malick A. Martuza, RL Inhibition of angiogenesis and growth of human nerve-sheath tumors by AGM-1470. J Neurosurg 1993;78:470–476. [PubMed: 8433151]
10. Emoto M, Tachibana K, Iwasaki H, Kawarabayashi T. Antitumor effect of TNP-470, an angiogenesis inhibitor, combined with ultrasound irradiation for human uterine sarcoma xenografts evaluated using contrast color Doppler ultrasound. Cancer Sci 2007;98:929–935. [PubMed: 17433035]
11. Nahari D, et al. Tumor cytotoxicity and endothelial Rac inhibition induced by TNP-470 in anaplastic thyroid cancer. Mol Cancer Ther 2007;6:1329–1337. [PubMed: 17431111]

12. Kanamori M, Yasuda T, Ohmori K, Nogami S, Aoki M. Genetic analysis of high-metastatic clone of RCT sarcoma in mice, and its growth regression in vivo in response to angiogenesis inhibitor TNP-470. J Exp Clin Cancer Res 2007;26:101–107. [PubMed: 17550138]
13. Sin N, et al. The anti-angiogenic agent fumagillin covalently binds and inhibits the methionine aminopeptidase, MetAP-2. Proc Natl Acad Sci USA 1997;94:6099–6103. [PubMed: 9177176]
14. Zhang Y, Griffith E, Sage J, Jacks T, Liu J. Cell cycle inhibition by the anti-angiogenic agent TNP-470 is mediated by p53 and p21WAF1/CIP1. Proc Natl Acad Sci USA 2000;97:6427–6432. [PubMed: 10841547]
15. Mauriz J, et al. Cell-cycle inhibition by TNP-470 in an in vivo model of hepatocarcinoma is mediated by a p53 and p21WAF1/CIP1 mechanism. Transl Res 2007;149:46–53. [PubMed: 17196522]
16. Kruger E, Figg WD. TNP-470: an angiogenesis inhibitor in clinical development for cancer. Expert Opin Investig Drugs 2000;9:1383–1396.
17. Kudelka A, Verschraegen C, Loyer E. Complete remission of metastatic cervical cancer with the angiogenesis inhibitor TNP-470. N Engl J Med 1998;338:991–992. [PubMed: 9527612]
18. Tran H, et al. Clinical and pharmacokinetic study of TNP-470, an angiogenesis inhibitor, in combination with paclitaxel and carboplatin in patients with solid tumors. Cancer Chemother Pharmacol 2004;54:308–314. [PubMed: 15184994]
19. Kudelka A, et al. A phase I study of TNP-470 administered to patients with advanced squamous cell cancer of the cervix. Clin Cancer Res 1997;3:1501–1505. [PubMed: 9815836]
20. Herbst R, et al. Safety and pharmacokinetic effects of TNP-470, an angiogenesis inhibitor, combined with paclitaxel in patients with solid tumors: evidence for activity in non-small-cell lung cancer. J Clin Oncol 2002;20:4440–4447. [PubMed: 12431966]
21. Stadler W, et al. Multi-institutional study of the angiogenesis inhibitor TNP-470 in metastatic renal carcinoma. J Clin Oncol 1999;17:2541–2545. [PubMed: 10561320]
22. Logothetis C, et al. Phase I trial of the angiogenesis inhibitor TNP-470 for progressive androgen-independent prostate cancer. Clin Cancer Res 2001;7:1198–1203. [PubMed: 11350884]
23. Bhargava P, et al. A phase I and pharmacokinetic study of TNP-470 administered weekly to patients with advanced cancer. Clin Cancer Res 1999;5:1989–1995. [PubMed: 10473076]
24. Satchi-Fainaro R, et al. Targeting angiogenesis with a conjugate of HPMA copolymer and TNP-470. Nat Med 2004;10:255–261. [PubMed: 14981512]
25. Cretton-Scott E, Placidi L, McClure H, Anderson D, Sommadossi J. Pharmacokinetics and metabolism of O-(chloroacetyl-carbamoyl) fumagillol (TNP-470, AGM-1470) in rhesus monkeys. Cancer Chemother Pharmacol 1996;38:117–122. [PubMed: 8616900]
26. Kataoka K, Harada A, Nagasaki Y. Block copolymer micelles for drug delivery: design, characterization and biological significance. Adv Drug Deliv Rev 2001;47:113–131. [PubMed: 11251249]
27. Harris J, Chess R. Effect of pegylation on pharmaceuticals. Nat Rev Drug Discov 2003;2:214–221. [PubMed: 12612647]
28. Edlund U, Albertsson A. Degradable polymer microspheres for controlled drug delivery. Adv Polym Sci 2001;157:67–112.
29. Rogers M, Birsner A, D'Amato R. The mouse cornea micropocket angiogenesis assay. Nat Protoc 2007;2:2545–2550. [PubMed: 17947997]
30. Carter, R.; Morton, A.; Dunnett, S. Motor coordination and balance in rodents. In: Taylor, G., editor. Current Protocols in Neuroscience. Vol. 8.12. John Wiley & Sons, Inc; New York: 2001. p. 1-8.
31. Almog N, et al. Prolonged dormancy of human liposarcoma is associated with impaired tumor angiogenesis. FASEB J 2006;20:947–949. [PubMed: 16638967]
32. Marler J, et al. Increased expression of urinary matrix metalloproteinases parallels the extent and activity of vascular anomalies. Pediatrics 2005;116:38–45. [PubMed: 15995028]
33. Folkman, J.; Klement, G. Platelet biomarkers for the detection of disease. US and International Patent. 20060204951. 2006.
34. Cervi D, et al. Platelet-associated PF-4 as a biomarker of early tumor growth. Blood. 2007
35. Kwon, Y. Handbook of Essential Pharmacokinetics, Pharmacodynamics and Drug Metabolism for Industrial Scientists. Plenum; New York: 2001.

36. Pierri E, Avgoustakis K. Poly(lactide)-poly(ethylene glycol) micelles as a carrier for griseofulvin. J Biomed Mater Res A 2005;75:639–647. [PubMed: 16110497]

37. Kakizawa Y, Kataoka K. Block copolymer micelles for delivery of gene and related compounds. Adv Drug Deliv Rev 2002;54:203–222. [PubMed: 11897146]

38. Torchilin V. Targeted polymeric micelles for delivery of poorly soluble drugs. Cell Mol Life Sci 2004;61:2549–2559. [PubMed: 15526161]

39. Nishiyama N, Kataoka K. Current state, achievements, and future prospects of polymeric micelles as nanocarriers for drug and gene delivery. Pharmacol Ther 2006;112:630–648. [PubMed: 16815554]

40. Barbera-Guillem E, Smith I, Weiss L. Cancer-cell traffic in the liver. I Growth kinetics of cancer cells after portal-vein delivery. Int J Cancer 1992;52:974–977. [PubMed: 1459739]

41. Greish K. Enhanced permeability and retention of macromolecular drugs in solid tumors: a royal gate for targeted anticancer nanomedicines. J Drug Target 2007;15:457–464. [PubMed: 17671892]

42. Duncan R. Polymer conjugates as anticancer nanomedicines. Nat Rev Cancer 2006;6:688–701. [PubMed: 16900224]

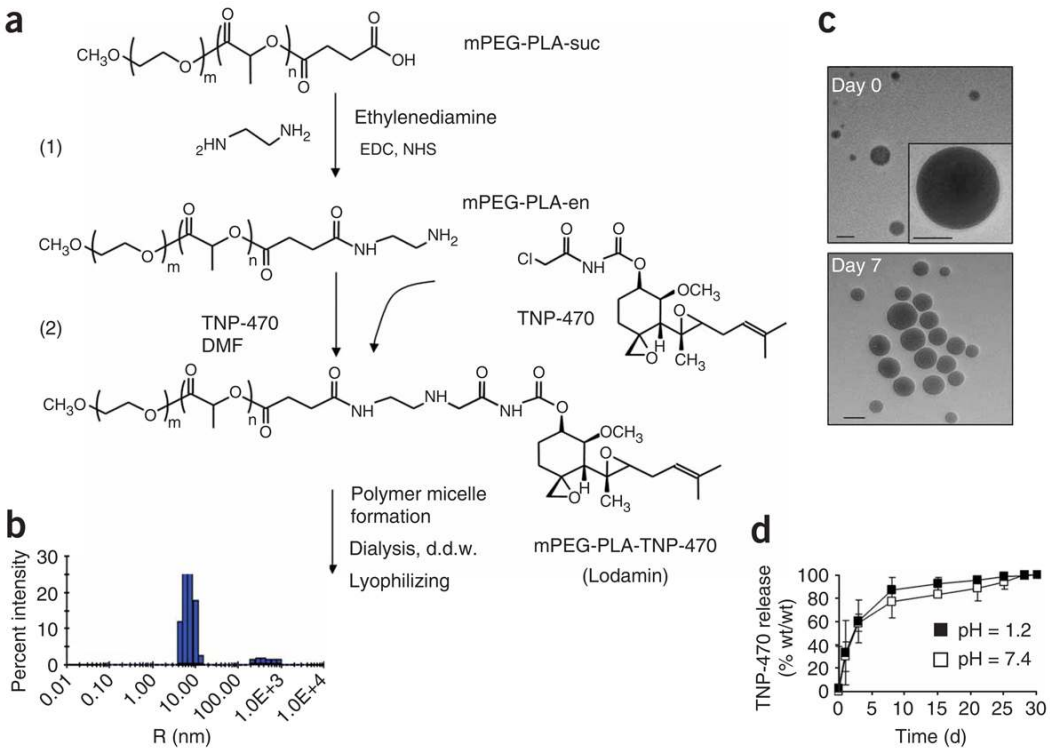

Figure 1.

Lodamin synthesis and characterization. (**a**) Diagram of the conjugation reaction between TNP-470 and modified mPEG-PLA. 1. The reaction between succinated mPEG-PLA and ethylendiamine that results in an amine-terminated polymer. 2. The reaction between the amine-containing polymer and the terminal chlorine of TNP-470. The conjugate is then dialyzed against water in an excess of TNP-470 to form polymeric micelles. (**b**) A typical DLS measurement of Lodamin, the graph shows size distribution of the polymeric-micelles in water. (**c**) TEM images of Lodamin dispersed in water, the spherical structure of the micelles are shown at different time points after incubation in water. Scale bar, 10 nm. (**d**) TNP-470 release from Lodamin during a 30-d period as determined by HPLC; micelles were incubated in gastric fluid pH = 1.2 or PBS pH = 7.4 and analysis of the released TNP-470 was done in duplicate. The results are presented as means ± s.d. mPEG-PLA, methoxy-polyethylene glycol–polylactic acid; suc, succinated; EDC, ethyl(diethylaminopropyl) carbodiimide; NHS, *N*-hydroxysuccinimide; en, ethylenamine; d.d.w., double-distilled water; DMF, dimethylformamide.

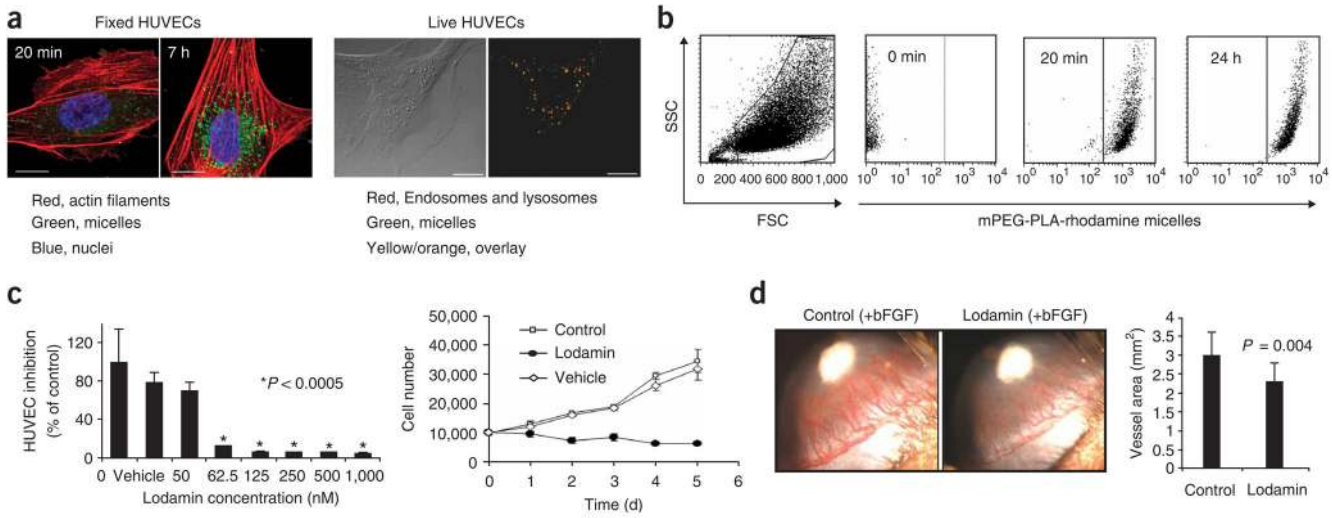

Figure 2.

Effect of Lodamin on angiogenesis and cell uptake of the drug. (**a**) Left: Confocal images show HUVEC uptake of polymeric micelles labeled with 6-coumarin after 20 min and 7-h incubation time periods. Right: Live HUVECs imaged 1 h after the addition of labeled micelles to cell medium (15 μg/ml, in green). LysoTracker Red detecting endosomes and lysosomes is shown in red. Overlay between micelles and endosomes/lysosomes is represented in yellow/orange color. Scale bars, 5 μm. (**b**) Uptake of rhodamine-labeled mPEG-PLA micelles by HUVECs was evaluated by FACS analysis. A viable cell gate was established based on forward and side scatter (FSC and SSC), and another gate was set for SSC/FL4$_{high}$-measurement of HUVECs containing mPEG-PLA-rhodamine micelles. Graphs of 0 min, 20 min and 24 hr of incubation with micelles are shown. Incubation after 2, 4 and 7 h showed a similar pattern as after 24 h of incubation (not shown). (**c**) HUVEC growth and proliferation. Upper panel: inhibition of HUVEC proliferation by different concentrations of Lodamin 50–1,000 nM TNP-470 equivalent. Empty polymeric micelles were also added as a control ($n = 8$, $^*P < 0.0005$). Lower panel: HUVEC growth curve of cells treated every other day with Lodamin (60 nM TNP-470 equivalent), untreated cells and vehicle-treated cells. (**d**) Corneal micropocket assay: representative experiments of the corneal micropocket assay. Newly formed blood vessels are growing toward the bFGF pellet (in white); note the inhibition of angiogenesis in Lodamin-treated mouse (15 mg/kg per day) with respect to control. Lower panel shows the quantification of neovascularization area in the cornea ($n = 10$, mean ± s.d.).

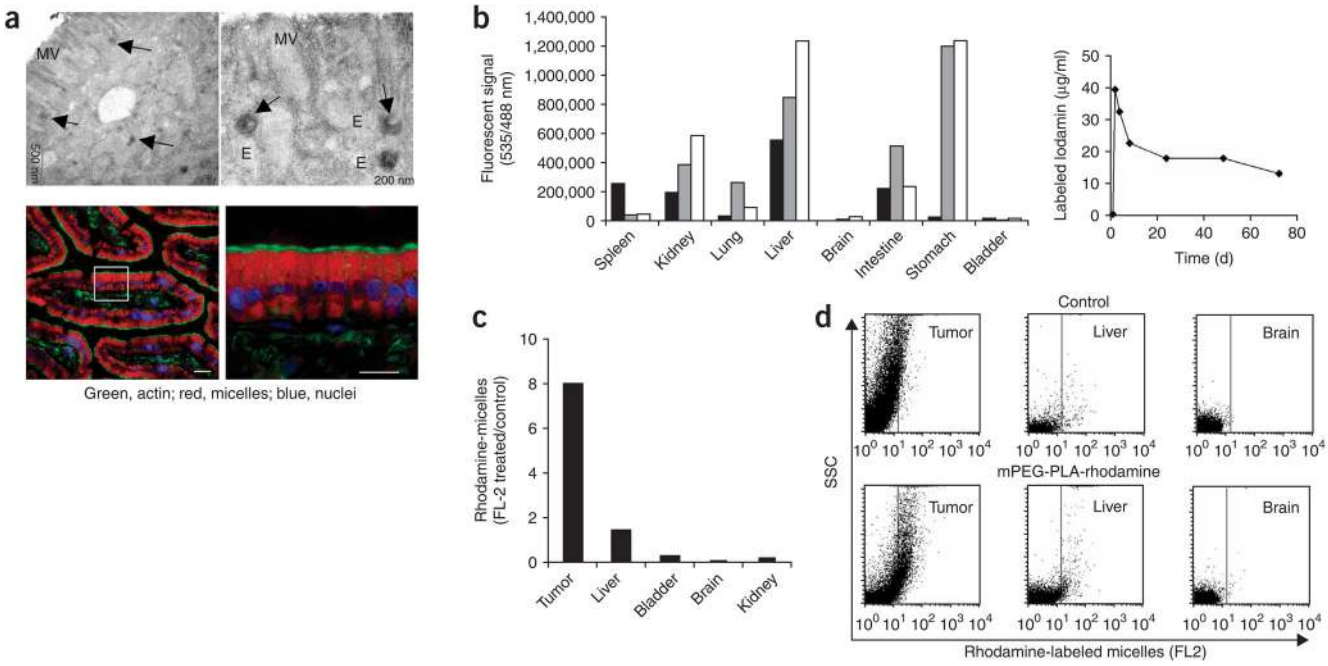

Figure 3.

Intestinal absorption and body distribution studies. (**a**) Intestinal absorption of mPEG-PLA micelles. Left, above: A histological section of gut epithelial cells of Lodamin-treated mouse observed with TEM. Microvilli (MV) structures and endosomes loaded with polymeric micelles (E, arrows) are detected. Scale bar, 500 nm (left) and 200 nm (right). Below: Confocal microscopy image. Note that the polymeric micelles can be detected in the lamina propria in the vicinity of blood vessels. The actin filaments were stained with phalloidin-FITC (green), nuclei were labeled with DAPI (blue) and mPEG-PLA-rhodamine micelles were detected in red. Scale bars, 5 μm. (**b**) Fluorescent signal of tissue extracts and in serum. Mice ($n = 3$) were given a single dose of oral 6-coumarin–labeled polymeric micelles (150 μl, 30 mg/ml). Left: the graph shows the values of the three different mice, autofluorescence was omitted by subtracting the fluorescent signal of tissue extracts from an untreated mouse. The percent of labeled cells was measured for each organ. Right: levels of fluorescent signals in mouse serum as measured after different time points after oral administration. The results are presented as the concentration of micelles calculated by standard calibration curve. (**c**) The percentage of $FL2^{high}$-positive cells is shown as isolated from the designated organs (ratio of numbers $FL2^{high}$ cells of treated tumors to these of control mouse). (**d**) FACS analysis graphs of single-cell suspensions from three representative organs (tumor, liver, brain) taken from a mouse bearing Lewis lung carcinoma after controlled enzymatic degradation. The $FL2^{high}$ represents those cells that contain the mPEG-PLA-rhodamine micelles.

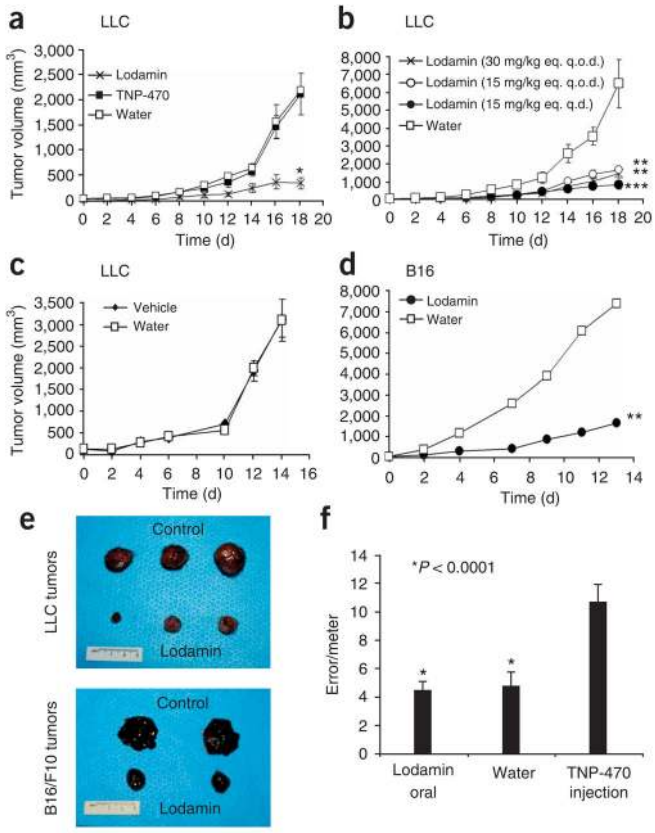

Figure 4.

Lodamin inhibits primary tumor growth without causing neurotoxicity. (**a**) Effect of free or conjugated TNP-470 on established Lewis lung carcinoma tumors: effect of 30 mg/kg every other day of free TNP-470 given orally, compared to equivalent dose of Lodamin or water ($n = 5$ mice per group, $^*P < 0.05$). (**b**) Lewis lung carcinoma volume during 18 d of different frequencies and doses of Lodamin: 30 mg/kg every other day (q.o.d.), 15 mg/kg every other day, 15 mg/kg every day (q.d.) and water by gavage ($n = 5$ mice per group, $^*P < 0.05$. (**c**) Evaluation of the effect of the vehicle, empty mPEG-PLA micelles, on Lewis lung carcinoma ($n = 5$ mice per group, $^*P < 0.05$). (**d**) Effect of Lodamin given at a dose of 15 mg/kg every day on B16/F10 murine melanoma tumor in C57Bl/6J, water was given as control ($n = 5$ mice per group, $^*P < 0.05$). (**e**) Representative Lewis lung carcinoma and B16/F10 tumors removed from mice at day 18 after treatment with oral Lodamin at 30 mg/kg every other day and 15 mg/kg every day, respectively, and from control untreated mice. (**f**) Neurotoxicity evaluation of Lodamin-treated mice (10 d, 30 mg/kg every other day) compared to mice treated with subcutaneous (30 mg/kg every other day) free TNP-470 or water given by gavage. Balance beam test was quantified by foot-slip errors and the numbers of slips per meter are presented ($n = 4$–5 mice per group). $^*P < 0.05$, $^{**}P < 0.01$, $^{***}P < 0.0001$ (results are mean ± s.e.m.).

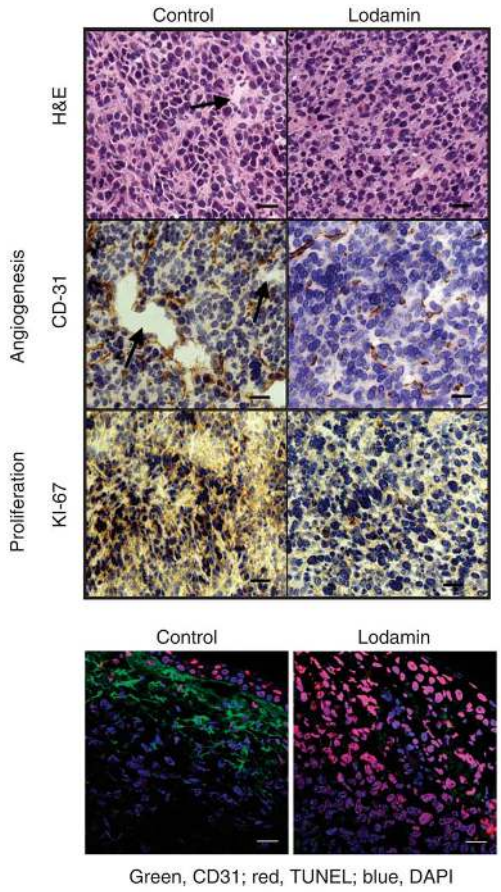

Figure 5.

Lodamin effect on tumor structure, cell proliferation, angiogenesis and apoptosis. Lewis lung carcinoma (LLC) tumors were removed from Lodamin-treated or untreated mice and sectioned. Tissues were stained with H&E to detect tissue morphology. Immunostaining with anti-CD31 was used to detect microvessels and anti-Ki-67 nuclear antigen for cell proliferation. TUNEL staining was used for the detection of apoptotic cells in lower panels. Vessels are detected in green, apoptotic cells are detected in red by TUNEL and cell nuclei are in blue (DAPI). Sections were counterstained with eosin (nuclei). Arrows indicate vessel structures. Scale bars, 15 μm.

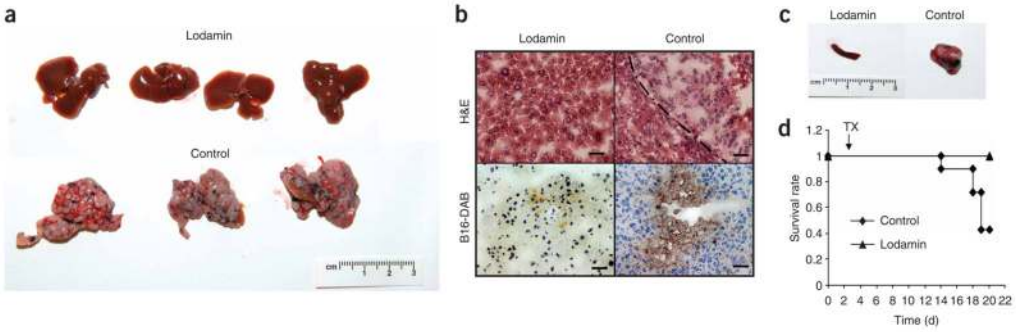

Figure 6.

Lodamin inhibits liver metastasis in mice injected with B16/F10 cells into their spleen. (**a**) Livers removed from Lodamin-treated or untreated mice, 20 d after cell injection. Control livers were enlarged with widespread macroscopic malignant nodules and extensive cirrhosis. (**b**) Histology of liver tissues. Livers removed from Lodamin-treated or untreated mice stained with H&E (upper panel) or reacted with anti-mouse melanoma antibody (lower panel). B16/F10 melanoma cells are detected by positive DAB staining (brown). (**c**) Spleens removed from Lodamin-treated or untreated mice. Control spleens had large masses compared to treated mice with normal spleen morphology. (**d**) Survival curve of treated versus control mice ($n = 7$). Treatment started at day three (TX) after cell injection (arrow).